Bull Volcanol (1992) 55:1-16

Bulletin of Volcanology

Petrology of lavas from episodes 2–47 of the Puu Oo eruption of Kilauea Volcano, Hawaii: evaluation of magmatic processes

MO Garcia[1], JM Rhodes[2], EW Wolfe[3], GE Ulrich[4], and RA Ho[1]

[1] Department of Geology and Geophysics, University of Hawaii, Honolulu, HI 96822, USA
[2] Department of Geology and Geography, University of Massachusetts, Amherst, MA 01003, USA
[3] US Geological Survey, 5400 MacArthur Blvd, Vancouver, WA 98661, USA
[4] US Geological Survey, 4472 Deer Trail, Sarasota, FL 34238, USA

Received December 30, 1991/Accepted June 1, 1992

Abstract. The Puu Oo eruption of Kilauea Volcano in Hawaii is one of its largest and most compositionally varied historical eruptions. The mineral and whole-rock compositions of the Puu Oo lavas indicate that there were three compositionally distinct magmas involved in the eruption. Two of these magmas were differentiated (<6.8 wt% MgO) and were apparently stored in the rift zone prior to the eruption. A third, more mafic magma (9–10 wt% MgO) was probably intruded as a dike from Kilauea's summit reservoir just before the start of the eruption. Its intrusion forced the other two magmas to mix, forming a hybrid that erupted during the first three eruptive episodes from a fissure system of vents. A new hybrid was erupted during episode 3 from the vent where Puu Oo later formed. The composition of the lava erupted from this vent became progressively more mafic over the next 21 months, although significant compositional variation occurred within some eruptive episodes. The intra-episode compositional variation was probably due to crystal fractionation in the shallow (0.0–2.9 km), dike-shaped (i.e. high surface area/volume ratio) and open-topped Puu Oo magma reservoir. The long-term compositional variation was controlled largely by mixing the early hybrid with the later, more mafic magma. The percentage of mafic magma in the erupted lava increased progressively to 100% by episode 30 (about two years after the eruption started). Three separate magma reservoirs were involved in the Puu Oo eruption. The two deeper reservoirs (3–4 km) recharged the shallow (0.4–2.9 km) Puu Oo reservoir. Recharge of the shallow reservoir occurred rapidly during an eruption indicating that these reservoirs were well connected. The connection with the early hybrid magma body was cut off before episode 30. Subsequently, only mafic magma from the summit reservoir has recharged the Puu Oo reservoir.

Correspondence to: MO Garcia

Introduction

The long-lived (since 1983, and continuing through mid-1992) Puu Oo eruption has been the most voluminous (>1.4 km^3) and one of the most compositionally variable among the historical eruptions of Kilauea Volcano. A multi-disciplinary approach has been utilized to help understand the processes associated with this eruption. This includes field observations, petrology of lavas, gas chemistry, seismicity, surface deformation, geoelectric observations and mechanics of eruption for the first 20 episodes of the eruption (see Wolfe 1988). In addition, measurement and analysis of ground deformation for episodes 22–42 permit inference of the geometry of the Puu Oo magma reservoir (see Hoffmann et al. 1990). These studies, carried out in the context of systematic eruption monitoring by the staff of the Hawaiian Volcano Observatory, have made the Puu Oo eruption Kilauea's most thoroughly documented eruption.

In this paper we present the results of a detailed petrologic study of the lavas from eruptive episodes 2–47. During this 3.8-year period, there were substantial compositional variations in the erupted lava. The short-term variations during an eruptive episode were largely caused by up to 5% fractionation in a shallow magma chamber beneath Puu Oo during repose periods. The long-term compositional variation reflects the progressive increase in the proportion of mafic magma, intruded just prior to the start of the eruption, mixed with a hybrid magma formed from two evolved magmas that were already at the site and were erupted during the first episode of the Puu Oo eruption.

Regional geology/eruption history

The basic magmatic reservoir system of Kilauea Volcano has been delineated by several studies (e.g. Ryan et al. 1981; Klein et al. 1987). A central conduit from the mantle supplies the summit reservoir with about 0.1 km^3 of magma per year. In the summit reservoir, magma is temporarily stored before being erupted at the summit

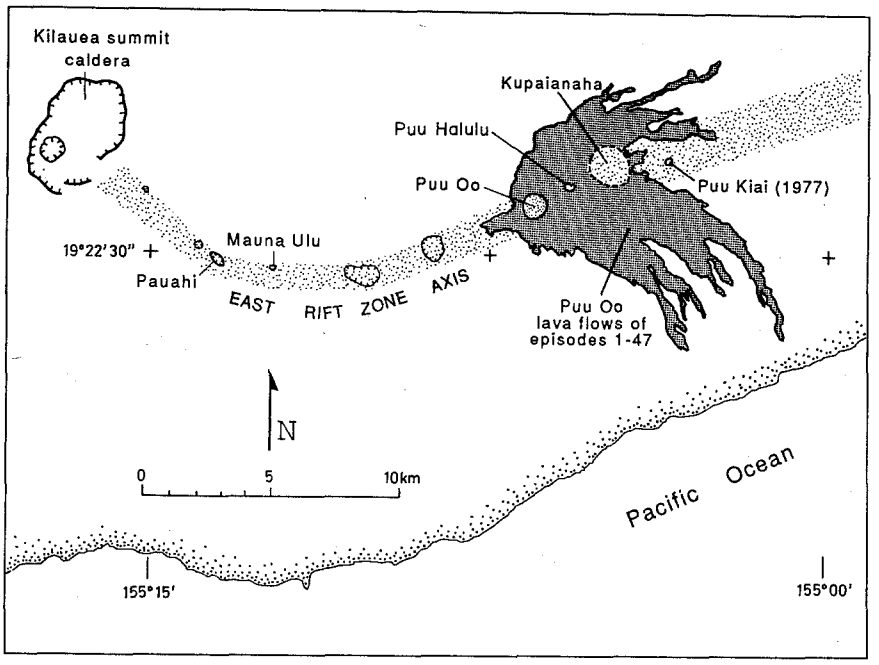

Fig. 1. Location map for the lavas (*dark stippled pattern*) and some vents related to episodes 1–47 of the Puu Oo eruption. The axis of the east rift zone of Kilauea is shown by the *light stippled pattern*. Depression, including the summit caldera, are indicated by *hatchured lines*. The other features shown along the rift zone are constructional highs formed by recent eruptions (Mauna Ulu, 1969–1974; Puu Kiai, 1977; Kupaianaha, 1986 to present)

or injected into the east or southwest rift zones (Dzurisin et al. 1984). Some magma from the central conduit may be injected into the deeper portions of the rift zones (6–10 km), bypassing the summit reservoir (Ryan 1988; Delaney et al. 1990). The details of the magma-conduit system are poorly known, but studies of eruption sequences (e.g. 1969–1974 eruptions; Ryan et al. 1981) have provided us with glimpses into its operation.

The vents for the Puu Oo eruption are located in the middle section of the Kilauea's east rift zone (Fig. 1). This region of the rift zone was a locus of repeated intrusion following its previous eruption in 1977. Evidence from seismicity and ground deformation (Klein et al. 1987; Wolfe et al. 1987) indicates that a pocket of magma formed in the area of the rift zone where Puu Oo later developed. During this period of frequent intrusions, there were two brief (<1 day) upper east rift eruptions (in 1979 at Pauahi Crater and in 1980 near Mauna Ulu), and two brief summit eruptions (in April and September of 1982).

The Puu Oo eruption was triggered by intrusion of a dike from the upper east rift zone into the middle section of the rift zone on 2 January 1983 (Wolfe et al. 1987). About 24 h later, the Puu Oo eruption started. It produced a 7.5-km long, discontinuous fissure that erupted along one segment or another, generally for 1–12 h, between 3 and 23 January. These episode-1 lavas are almost entirely hybrids produced by mixing two rift-zone-stored, differentiated magmas in varying proportions (Garcia et al. 1989). Following a 17-day break in eruptive activity, when only burning gas and small amounts of spatter were produced, lava issued from four vents along a 1.1-km section of the fissure system during episode 2 (Wolfe et al. 1988). Most of the lava erupted came from the 1123 vent (renamed Puu Halulu; Fig. 1). The O vent (since renamed Puu Oo) produced lava intermittently for only about 41 h of the 22-day, episode-2 eruption, but regrettably none was sampled. Lava from episode 3 erupted from only two vents, most of it from Puu Halulu, although Puu Oo produced a 5-km long flow. For episodes 4–47, lava was erupted almost exclusively from the Puu Oo vent. A spatter cone, Puu Oo, formed around the vent and grew to 255 m above the original surface by the end of episode 47. During some eruption episodes (4, 11, 21, 25, 28, 29, 35 and 44), lavas erupted from fissures at the base of the cone, which were oriented parallel to the strike of the rift zone (~N65° E).

At the start of episode 48, new eruptive fissures formed just uprift (SW) and downrift (NE) from Puu Oo. Another fissure formed two days later about 3 km downrift of Puu Oo, and this became the site of virtually continuous eruptive activity (the Kupaianaha vent) (Heliker and Wright 1991) until November 1991.

The eruptive activity at the Puu Oo vent was cyclical. Repose periods between eruptive episodes 2–47 varied from 8 days (between episodes 8 and 9 and 13 and 14) to 65 days (between episodes 3 and 4), although 83% lasted from 17 to 39 days. During episodes 3–47, the duration of vigorous eruptive activity ranged between 5 h (episode 26) and 384 h (for the episode-35 fissure eruptin). The early episodes (2–20) were generally longer (19–290 h) than the later episodes (21–47; 5–21.5 hours), except for the episode-35 fissure eruption.

After episode 1, Kilauea's reservoir system inflated gradually during repose periods of Puu Oo and deflated rapidly during eruptive episodes. These alternating inflations and deflations were roughly equivalent in magnitude. This implies that the long-term discharge of magma from Puu Oo approximately equaled the supply of new magma to the reservoir system. Lava-volume measurements, corrected for porosity, indicate that over the 3-1/2 years of episodic eruptions, magma was erupted from Puu Oo at an average rate of about 14000 m^3 per

hour through at least episode 20 (Wolfe et al. 1987). However, changes in eruption style during this period reflected an increasingly efficient linkage between Kilauea's summit reservoir and the Puu Oo vent. These changes included increasing rates of lava production in successive episodes (80000–1760000 m^3 per hour) and correspondingly shorter eruption periods (175–9 h, excluding anomalous episodes). The higher eruption rates were also reflected by greater heights of fountaining. In addition, the duration of repose periods between eruptive episodes became more systematic and predictable.

Petrography

Nearly all samples used in this study were collected molten near the Puu Oo vent from active flows or fresh spatter. A few tephra samples were collected 1–1.5 km downwind from the vent. Lava samples were collected near the vent (usually <1 km; see Table 1) to minimize compositional changes caused by flow segregation of phenocrysts (e.g. Fuller 1939). Most were water-quenched to minimize post-eruptive crystallization. These samples are glassy, strongly vesicular, and friable. Additional information for samples collected from episodes 1 to 20 is given by Neal et al. (1988).

Puu Oo lavas are predominantly aphyric (<1 vol % phenocrysts), especially those erupted after episode 10 (Table 1). Thus, the lava compositions closely approach those of liquids. The modes of the lavas systematically changed during the overall eruption (episodes 1–47) and during some individual eruptive episodes (Garcia and Wolfe 1988). Lava from the early Puu Oo eruptions (episodes 1–4 and early parts of episodes 5–10) contains plagioclase and clinopyroxene (mostly as microphenocrysts, 0.1–0.5 mm) (Table 1). Lava from later episodes (11–47) contains no phenocrysts of plagioclase or clinopyroxene (except sample 25-315) and only rarely contains sparse (<0.2 vol %) microphenocrysts of these phases. Small (0.1–1.0 mm) olivines are present in all of the samples studied, but are rare (<0.1 vol %) in some (Table 1). Olivine phenocrysts (0.5–1.0 mm) are more abundant in samples from episodes 30 and 31 and the later portions of episodes 7–10. Inclusions of Cr-spinel are present in some olivines. Samples from some individual eruptive episodes (4–10) show systematic variations with time in modal olivine and plagioclase. Olivine increases and plagioclase decreases in abundance in successive samples collected during each of these episodes (Garcia and Wolfe 1988; Table 1).

Most of the minerals in the Puu Oo lavas are euhedral, but a few olivine, clinopyroxene and plagioclase grains are anhedral. Olivine in some early Puu Oo lavas, and clinopyroxene in some of the lavas from the later portions of episodes 5–10 are resorbed. Some of the euhedral plagioclase grains have irregular oscillatory zoning. Crystal clots composed of plagioclase and clinopyroxene, either with or without interstitial glass, are present in pre-episode 11 lavas.

Mineral chemistry

The compositions of minerals from representative Puu Oo lava samples were determined by electron microprobe. The operating conditions used for the University of Hawaii microprobe were 15 kV and 10 to 15 nA in a beam current regulated mode. A finely focused beam (1 μ wide) was used to examine compositional zoning in the minerals. Typically, each element was counted for 20 s. Raw data were corrected using ZAF procedures. The values reported in Tables 2–4 are averages of at least three spot analyses/grain. Previously reported analyses for Puu Oo lavas include the compositions of olivine cores from a few samples from episodes 3–12, clinopyroxene cores from two samples from episodes 7 and 8 (Garcia and Wolfe 1988), and the core and rim composition of olivine, clinopyroxene and plagioclase microphenocrysts from four episode 1 lavas (Garcia et al. 1989).

Olivine

The compositions of olivine cores from episodes 3 through 47 range widely (Fo 74–88, Table 2, Fig. 2). Within some individual samples there are wide ranges in core composition, especially in the late lavas from episodes 3 and 9. These variations extend both above and below the olivine-liquid equilibrium field (Fig. 2). This is surprising given the low phenocryst content of most of the samples (i.e. the bulk composition of the lava should closely approximate the liquid composition) and the small grain size of most of the olivines (0.1–0.6 mm). However, the crystals with core compositions that plot below the equilibrium field (Fig. 2) usually are resorbed or anhedral. These grains also exhibit reverse zoning (Fig. 3). The magnitude of the reversals is small (1–2% Fo), but the trends are consistent. The width of the reverse zones varies from 50–120 μ (Fig. 3). These grains have compositions similar to those of olivine from the most evolved lavas of episode 1 (Fig. 2). In contrast, olivines in episode 48 lavas (from Kupaianaha vent) have narrow compositional ranges that plot within the equilibrium field (Fig. 2).

Olivine in the samples with higher forsterite contents displays normal zoning. The four grains with very high forsterite content (87–88%) in the two late episode 9 lavas would not have been in equilibrium with any Puu Oo lava yet erupted (including the slightly more mafic lavas erupted from the later Kupaianaha vent). Although these grains are euhedral, they are probably xenocrysts. The other grains that plot above the equilibrium field could have been derived from the mafic endmember of Puu Oo lavas, which would have had equilibrium olivines with forsterite contents of 84–86.5%.

Clinopyroxene

Most of the analyzed grains are microphenocrysts; all are <0.6 mm across (Table 2). Optical zoning is common. Most grains have oscillatory zoning; some also

Table 1. Modes in volume % for volcanic rocks from episodes 2–47 of the Puu Oo eruption. Based on 1000 counts per sample (* except for frothy samples, which have 500 counts). Day is the cumulative total of days since the start of the Puu Oo eruption on 3 January 1983. Distance indicates how many meters (m) from its vent sample was collected; *FISS*, from fissure eruption on flank of Puu Oo. Rock types: *F*, flow, *S*, spatter, *T*, tephra. Method of quenching sample: H_2O (water), or air. Phenocrysts (*Ph*) are larger than 0.5 mm; microphenocrysts (*Mph*) are 0.1–0.5 mm in size. Analysts: E Matsumoto; M Garcia

Episode Sample	Date	Day	Distance	Type	Quench	Olivine		Clinopyroxene		Plagioclase		Matrix
						Ph	Mph	Ph	Mph	Ph	Mph	
2- 66*	16-Feb-83	45	30	F	H_2O	0.2	0.2	0	2.8	0.2	3.6	93.0
2- 77*	25-Feb-83	54	120	F	H_2O	0	0.2	0	2.4	0	2.4	95.0
2- 81*	01-Mar-83	58	0	S	H_2O	0	0.2	0.2	0.8	0	1.6	97.2
3- 88	28-Mar-83	85	150	F	H_2O	0.2	0.5	0.3	4.2	0.5	6.1	88.2
3- 96	31-Mar-83	88	300	F	H_2O	0	0.3	0	0.4	1.0	2.0	96.3
3-117*	09-Apr-83	97	200	F	?	0.4	0.2	0	<0.1	0.4	2.0	97.0
4-121*	13-Jun-83	162	30	F	H_2O	0.2	0.2	0	3.6	0.2	2.6	93.2
4-130*	17-Jun-83	166	1100	F	H_2O	1.6	0.8	0	4.4	0	0.4	92.8
5-136*	29-Jun-83	178	70	F	H_2O	0.4	0.2	0.6	2.4	0.2	1.4	94.8
5-139*	03-Jul-83	182	< 50	F	Air	0.6	1.1	0	0.6	0	0.5	97.2
6-146*	22-Jul-83	201	0	F	H_2O	0	0.2	0	2.0	0.2	3.6	94.0
6-154	26-Jul-83	205	100	F	H_2O	0.8	1.5	0	1.5	0	<0.1	96.2
7-159*	15-Aug-83	225	~1000	F	H_2O	0	0.6	0	1.8	0	0.4	97.2
7-162*	15-Aug-83	225	300	F	H_2O	1.0	0.8	0	1.4	0	0.2	96.6
7-163*	16-Aug-83	226	250	F	H_2O	0.4	1.0	0	1.6	0	<0.1	97.0
7-167*	17-Aug-83	227	900	F	H_2O	3.4	1.4	0	0.4	0	0	94.8
8-172	06-Sept-83	247	850	F	H_2O	0.2	0.2	0	1.5	0	<0.1	98.1
8-174*	07-Sept-83	248	30	F	Air	1.9	2.4	0	0.9	0	<0.1	94.8
9-175	15-Sept-83	256	30	F	H_2O	0	1.4	0	0.8	0	0.8	97.0
9-178*	23-Sept-83	264	25	F	Air	3.5	2.1	0	0.2	0	<0.1	94.2
10-179	02-Oct-83	273	< 10	F	?	<0.1	1.9	0	1	0	1.1	96.0
10-183*	05-Oct-83	276	1200	F	H_2O	0	0.6	0	1.5	0	0	97.9
10-187	07-Oct-83	278	1600	F	H_2O	2.1	2.3	0	0.2	0	0	95.4
11-195*	07-Nov-83	309	250	F	Air	0	0.5	0	0.3	0	0	99.2
12-196	30-Nov-83	332	250	F	H_2O	0	0.5	0	0	0	0	99.5
12-197*	30-Nov-83	332	600	F	H_2O	0	0.4	0	0.2	0	0	99.4
12-200	30-Nov-83	332	400	F	H_2O	0	0.3	0	0	0	0	99.7
12-201	01-Dec-83	333	200	F	H_2O	0	<0.1	0	0	0	0	99.9
12-202	01-Dec-83	333	600	F	Air	0.3	0.5	0	0	0	0	99.2
12-203	01-Dec-83	333	650	F	H_2O	0	1.3	0	0.3	0	<0.1	98.4
13-209	20-Jan-84	383	300	F	H_2O	0.5	0.4	0	0	0	<0.1	99.1
13-216	21-Jan-84	384	700	F	H_2O	0	0.1	0	<0.1	0	<0.1	99.9
13-224*	22-Jan-84	385	300	F	H_2O	0	<0.1	0	0	0	0	99.9
13-225*	22-Jan-84	385	250	F	H_2O	0	<0.1	0	0	0	0	99.9
14-229*	30-Jan-84	393	< 10	F	H_2O	1.2	0.2	0	0	0	<0.1	98.6
14-232*	31-Jan-84	394	150	F	H_2O	0.2	0.2	0	0	0	0	99.6
15-237*	15-Feb-84	409	~1000	F	Air	0.4	0	0	0	0	0	99.6
16-246*	02-Mar-84	425	< 10	S	H_2O	0.2	2.6	0	0	0	0	97.2
16-247*	03-Mar-84	426	300	F	H_2O	0	0.6	0	0	0	0	99.4
16-254*	04-Mar-84	427	1200	F	H_2O	0	1.8	0	<0.1	0	0	98.2
17-256*	30-Mar-84	453	~1000	F	H_2O	0	0.4	0	0	0	0.2	99.4
17-260	31-Mar-84	454	~2000	F	H_2O	<0.1	0.4	0	<0.1	0	0	100
18-263	19-Apr-84	473	500	F	H_2O	0.3	0.4	0	0	0	0	99.3
18-269	21-Apr-84	475	~2000	F	H_2O	0	0.6	0	0	0	0	99.4
20-274*	08-Jun-84	523	~4000	F	H_2O	0	0.6	0	0	0	0	99.4
22-283*	09-Jul-84	554	~1500	F	H_2O	0.2	0.4	0	0	0	0	99.4
25-315	19-Sep-84	626	0, FISS	F	H_2O	<0.1	0.1	0.1	0	0	0	99.8
25-325	04-Oct-84	641	< 100	F	Air	0.1	0.6	0	0	0	0	99.3
26-332	02-Nov-84	670	500	F	H_2O	0.1	0.2	0	0	0	0	99.7
26-333	02-Nov-84	670	< 50	F	Air	<0.1	0.2	0	0	0	0	99.8
28-337	04-Dec-84	702	~2000	F	H_2O	0	0.3	0	0	0	0	99.7
29-350	03-Jan-85	732	0, FISS	F	Air	0	0.6	0	0	0	0	99.4
29-356	17-Jan-85	746	< 50	F	Air	0	0.3	0	0	0	0	99.7
30-359	04-Feb-85	764	~1000	F	H_2O	0.1	0.8	0	0	0	0	99.1
30-361	06-Feb-85	766	7800	F	Air	1.0	2.1	0	0	0	0	96.9
30-362	08-Feb-85	768	15	S	Air	0.6	2.6	0	0	0	0	96.8
31-363	04-Mar-85	792	< 50	S	Air	0.8	1.6	0	0	0	0	97.6
31-367	13-Mar-85	801	~8000	F	Air	1.2	1.8	0	0	0	0	97.0
31-368	21-Mar-85	809	< 100	F	Air	1.4	1.2	0	0	0	0	97.4
32-370*	21-Apr-85	840	~1000	F	H_2O	0.6	1.0	0	0	0	0	98.4

Table 1 (continued)

Episode Sample	Date	Day	Distance	Type	Quench	Olivine		Clinopyroxene		Plagioclase		Matrix
						Ph	Mph	Ph	Mph	Ph	Mph	
35-394	26-Jul-85	936	?, FISS	F	Air	0.3	1.0	0	0	0	0	98.7
35-419*	30-Jul-85	940	0, FISS	S	Air	0.6	2.0	0	0	0	0	97.4
38-458*	21-Oct-85	1023	150	F	Air	0	0.2	0	0	0	0	99.8
40-484*	01-Jan-86	1095	200	F	H_2O	0	1.0	0	0	0	0	99.0
42-514	22-Feb-86	1147	1500	T	Air	0.4	2.2	0	<0.1	0	0	97.4
46-536*	02-Jun-86	1247	500	F	Air	0	2.4	0	<0.1	0	0	97.6
46-542*	02-Jun-86	1247	~1000	T	Air	0	3.0	0	0	0	0	97.0
46-549	02-Jun-86	1247	~1000	T	Air	0	1.0	0	0.4	0	0	98.6
47-570	26-Jun-86	1271	~1500	F	Air	0	0.5	0	0	0	0	99.5

have sector zoning. All of the grains have an augite composition, but some have CaO-poor cores or rims. The wollastonite component ranges from 40 to 27%, but most grains are in the range of 36–40%. The ferrosilite component ranges from 9 to 16%, but the majority of the grains (both cores and rims) are in the range of 10–13%. Both normally and reversely zoned grains are present, and both types are usually euhedral. Cores of normally zoned grains have lower ferrosilite content (<11%); the cores of reversely zoned grains all have greater ferrosilite contents, and, in many, opaque inclusions are common. In most of the reversely zoned grains, SiO_2, MgO, Cr_2O_3 and CaO contents increase and FeO, TiO_2 and Al_2O_3 contents decrease from core to the rim. The grains with CaO-poor cores show increasing TiO_2, Al_2O_3 and CaO and decreasing SiO_2, FeO and MgO contents from core to rim, but the ratio of MgO/FeO remains relatively constant. Lofgren (1980) suggested that such clinopyroxenes may be caused by the kinetics of crystal growth rather than magma mixing.

Plagioclase

Plagioclase phenocrysts and microphenocrysts in samples from episodes 3–9 have a large compositional range (An 61–79; Table 2). This range is typical for Kilauea (see Clague et al. 1992 for a summary). Many of the more sodic (An 60–70) Puu Oo plagioclase grains exhibit reverse zoning and are anhedral. The more calcic plagioclases (>An 70) all have normal zoning.

Spinel

Spinels occur only as inclusions in olivine in the Puu Oo lavas. As noted in studies of other Kilauea basalts (e.g. Wilkinson and Hensel 1988; Nicholls and Stout 1988), olivine in most Puu Oo lavas contains Cr-rich spinels (Cr_2O_3 = 34–42 wt %; Table 2). However, olivine in the most evolved lavas rarely contains spinel. Except for sample 3-88, the olivines in which spinels occur have a limited compositional range (Fo 81.6–85.2). There is a good correlation of the Mg content of the spinel and the forsterite content of the olivine. The Cr-spinels are relatively homogeneous (e.g. Al_2O_3, 11.5–15.0 wt %; MgO 9.8–11.6 wt %; TiO_2, 1.8–4.1 wt %); an exception is the rare spinel in evolved sample 3-88. The limited compositional range of the spinels probably reflects their early crystallization.

Whole-rock geochemistry

Representative lavas from throughout the Puu Oo eruption were analyzed by XRF at the University of Massachusetts for major and trace (Rb, Nb, Zr, Sr, Y, V, Zn, Ni and Cr) elements (Table 3). Samples were selected for XRF analysis on the basis of microprobe analyses of fused, whole-rock samples from a large suite of Puu Oo lavas (Garcia and Wolfe 1988). Multiple samples were analyzed from episodes with substantial compositional variation (3, 5–10, 30, 31). All samples were analyzed in duplicate using the methods outlined in Rhodes (1988).

There is a large range in composition for the Puu Oo lavas from episodes 2–47. For example, MgO ranges from about 5.9 to 9.5 wt % and TiO_2 from 2.35 to 3.03 wt % (Fig. 4). Generally, SiO_2, Al_2O_3, TiO_2, Na_2O, K_2O and P_2O_5 contents increase with decreasing MgO content, but there is more variation at a given MgO content than can be attributed to analytical error. MgO variations for total iron (as Fe_2O_3) and CaO have opposite trends, but each trend has an 'elbow' in the middle. Fe_2O_3 contents initially decrease with decreasing MgO to about 7.3 wt % MgO and then increase; CaO contents exhibit much more variation.

Among the trace elements, Ni and Cr contents decrease with decreasing MgO, and Rb, Nb, Y, V, Zn and Sr increase with increasing Zr (an incompatible element). There is considerable scatter on a Cr versus Zr plot (Fig. 5). Some of the scatter can be reconciled with a mixing trend between the least and most evolved lavas. The other trace elements define linear variation trends except for V, which deviates from a linear trend in the highest MgO content samples from episodes 30 and 31.

Table 2. Mineral analyses of representative Puu Oo lavas

Sample	3-88		3-97		9-175		9-178						10-187			
Olivine																
Size Portion	0.55		0.25*		0.40		0.25*		0.50		1.0		1.1		0.6	
	Core	Rim	Core	Rim	Core	Rim	Core	Rim	Core	Rim	Core	Rim	Core	Rim	Core	Rim
SiO_2	39.0	39.0	38.2	38.5	39.1	39.0	38.7	38.8	39.8	39.6	39.6	38.7	39.9	39.8	39.7	39.5
FeO	18.5	18.5	23.7	22.2	18.4	20.2	19.1	18.7	15.0	16.6	12.2	16.4	14.8	15.4	15.5	15.8
MgO	42.0	41.9	37.4	38.3	41.6	40.1	41.6	42.2	44.6	43.2	47.5	44.2	44.7	44.1	44.6	44.3
Total	99.5	99.4	99.3	99.0	99.1	99.3	99.4	99.7	99.4	99.4	99.3	99.3	99.4	99.3	99.8	99.6
Fo%	80.1	80.1	73.8	75.4	80.2	78.0	79.5	80.1	84.1	82.2	87.4	82.7	84.3	83.5	83.6	83.3
Clinopyroxene																
Size Portion	0.50*		0.60		0.40*		0.17*		0.38		0.782		0.40*		0.20*	
	Core	Rim	Core	Rim	Core	Rim	Core	Rim	Core	Rim	Core	Rim	Core	Rim	Core	Rim
SiO_2	52.9	52.6	52.4	51.7	51.0	52.3	50.8	51.9	52.7	52.2	52.6	51.8	51.5	52.1	51.5	51.5
TiO_2	0.7	0.7	0.7	1.0	1.7	0.8	1.5	0.8	0.7	0.9	0.6	0.7	0.9	0.8	1.0	0.8
Al_2O_3	2.1	2.3	2.2	2.9	3.6	2.5	3.3	2.9	2.2	2.8	2.4	3.0	3.3	2.6	2.1	3.1
Cr_2O_3	0.2	0.5	0.3	0.3	0.2	0.3	0.4	0.9	0.3	0.7	0.8	0.8	0.9	0.5	0.0	1.0
FeO	7.6	6.9	7.2	8.2	8.0	6.9	8.7	6.0	6.5	6.7	6.5	6.6	6.2	6.4	10.2	6.1
MgO	17.9	17.6	18.0	17.4	16.7	17.5	16.7	178.6	18.2	17.6	18.0	17.4	17.2	17.8	16.4	17.2
CaO	18.7	18.0	18.6	18.1	18.3	18.8	18.3	19.5	19.0	19.4	19.3	19.5	19.5	19.0	18.3	19.7
Na_2O	0.27	0.22	0.25	0.25	0.30	0.25	0.25	0.30	0.25	0.25	0.26	0.28	0.30	0.25	0.25	0.25
Total	100.37	99.82	99.65	99.85	99.80	99.35	99.95	99.90	99.85	100.55	100.46	100.08	99.8	99.45	99.75	99.65
Plagioclase																
Size Portion	1.10		0.75*		0.52*		0.1A									
	Core	Rim	Core	Rim	Core	Rim	Core									
SiO_2	49.1	50.4	52.7	51.5	50.8	48.6	51.1									
Al_2O_3	32.0	31.0	29.2	30.3	30.8	32.7	30.7									
Fe_2O_3	0.65	0.65	0.65	0.65	0.70	0.80	0.65									
MgO	0.15	0.15	0.20	0.20	0.20	0.15	0.20									
CaO	15.4	14.3	12.5	13.8	14.1	16.1	14.0									
Na_2O	2.45	3.2	3.8	3.4	3.1	2.0	3.0									
K_2O	0.10	0.15	0.10	0.10	0.10	0.10	0.10									
Total	99.85	99.85	99.15	99.95	99.80	100.45	99.75									
An%	75.6	70.0	61.2	67.3	68.9	78.7	68.4									
Spinel																
Size Portion	0.025							0.05R					0.006	0.002		
	Core							Core	Rim				Core	Core		
TiO_2	10.69							2.75	3.71				3.16	1.81		
Al_2O_3	11.48							11.49	14.07				14.56	12.39		
Cr_2O_3	21.09							43.08	35.62				35.55	44.23		
Fe_2O_3	18.34							11.67	14.21				14.19	10.74		
FeO	27.26							20.32	21.13				20.99	18.54		
MnO	0.26							0.26	0.29				0.27	0.28		
MgO	10.11							10.14	10.32				10.03	10.61		
Total	99.23							99.71	99.35				98.75	98.60		

Size of grains is in mm. All mineral grains are euhedral except as noted by a letter next to size: *A*, anhedral; *R*, round. Reversely zoned grains are noted with an *asterisk* next to the grain size. Fe_2O_3 content of spinel was recalculated from the total iron content of the analysis assuming stoichiometry. Analysts: J Hayes, R Ho and M Garcia

Temporal variation

Concentrations of all major elements except SiO_2 changed progressively for the first 500 days of the Puu Oo eruption and then remained relatively constant for the next 700 days (except during episodes 30 and 31 and for Fe_2O_3). CaO and MgO increase and TiO_2, Al_2O_3, Fe_2O_3, Na_2O, K_2O and P_2O_5 decrease progressively. This systematic variation is illustrated on the plot of CaO/TiO_2 (a ratio which is not affected by olivine frac-

Table 3. XRF major and trace element data for episode 2–47 lavas from the Puu Oo eruption. Samples are listed in chronologic order with the episode number followed by the sample number. Major elements are in wt %; trace elements in ppm. Total iron is given as Fe_2O_3. See Rhodes (1988) for a discussion of the methods used and for an estimate of analytical precision

Sample	SiO_2	TiO_2	Al_2O_3	Fe_2O_3	MnO	MgO	CaO	Na_2O	K_2O	P_2O_5	Y	Sr	Rb	Nb	Zr	Zn	Ni	Cr	V
2-066	50.44	3.109	13.67	12.73	0.18	5.91	9.97	2.62	0.665	0.343	30.9	401	11.9	23.2	223	130	92	96	336
2-077	50.47	3.115	13.76	12.71	0.17	5.95	10.04	2.66	0.652	0.340	30.5	401	11.4	22.8	220	130	92	97	335
2-081	50.42	3.025	13.93	12.49	0.17	6.02	10.25	2.55	0.624	0.321	29.2	400	10.9	21.9	209	126	94	122	329
3-088	50.20	2.830	13.74	12.30	0.17	6.60	10.48	2.49	0.570	0.294	27.5	389	10.4	21.7	191	123	115	202	318
3-096	50.44	3.020	13.96	12.49	0.18	5.94	10.24	2.72	0.628	0.320	29.6	406	11.8	23.1	210	127	94	120	330
3-117	50.57	3.029	13.96	12.55	0.17	6.06	10.27	2.59	0.616	0.324	29.4	401	10.9	21.8	206	124	93	118	314
4-121	50.36	2.722	13.69	12.11	0.17	7.03	10.65	2.45	0.540	0.283	26.7	378	9.5	20.1	182	119	132	301	311
4-130	50.12	2.745	13.56	12.16	0.17	7.07	10.49	2.39	0.564	0.287	27.3	372	9.8	21.3	185	122	137	295	311
5-136	50.23	2.730	13.65	12.10	0.17	6.98	10.67	2.30	0.543	0.282	27.2	370	9.9	19.2	181	118	125	293	309
5-139	49.85	2.568	13.13	12.22	0.17	8.10	10.46	2.30	0.504	0.260	26.5	356	8.3	18.4	167	119	190	432	302
6-146	49.79	2.716	14.39	12.11	0.17	6.63	10.74	2.41	0.547	0.277	27.1	374	9.0	20.4	178	119	112	267	311
6-154	50.19	2.592	13.12	12.26	0.17	8.28	10.54	2.38	0.503	0.267	25.3	355	8.7	17.4	168	121	170	425	292
7-159	50.09	2.687	13.57	12.03	0.17	6.78	10.81	2.39	0.530	0.277	26.7	370	8.9	20.0	174	119	121	282	306
7-162	50.35	2.678	13.65	12.06	0.17	7.03	10.81	2.44	0.527	0.279	26.8	368	9.3	19.4	183	117	122	296	303
7-163	50.02	2.628	13.31	12.14	0.17	7.60	10.65	2.27	0.514	0.272	25.9	358	9.1	17.8	179	117	154	358	301
7-167	49.51	2.590	13.55	12.19	0.17	7.85	10.59	2.23	0.518	0.265	25.7	351	8.9	17.4	173	—	199	419	297
8-172	50.39	2.664	13.59	11.98	0.17	6.94	10.90	2.34	0.526	0.274	26.5	366	9.1	19.1	177	122	122	293	308
8-174	50.16	2.571	13.19	12.19	0.17	7.94	10.68	2.24	0.499	0.260	25.8	354	8.5	17.2	167	114	174	404	292
9-175	50.85	2.652	13.66	12.01	0.16	7.17	10.96	2.32	0.524	0.274	26.5	366	9.1	18.6	179	118	118	288	302
9-178	50.16	2.550	13.12	12.15	0.18	8.19	10.69	2.31	0.497	0.260	25.5	352	8.5	16.6	167	115	182	451	294
10-179	50.19	2.633	13.58	12.02	0.17	7.01	11.08	2.28	0.507	0.266	26.1	362	8.6	17.7	175	118	124	316	308
10-183	50.24	2.609	13.44	12.08	0.17	7.15	11.02	2.24	0.515	0.265	25.4	359	8.7	18.4	169	119	125	329	307
10-187	49.73	2.508	13.04	12.15	0.17	8.39	10.64	2.27	0.489	0.254	25.3	346	8.2	17.1	165	115	182	446	295
11-195	50.50	2.581	13.46	12.01	0.17	7.28	11.09	2.26	0.495	0.260	26.1	357	8.4	17.1	170	115	128	332	296
12-196	50.10	2.566	13.34	11.95	0.17	7.17	11.09	2.23	0.500	0.261	25.5	359	8.4	18.1	168	115	124	322	298
12-197	50.04	2.566	13.31	11.98	0.17	7.23	11.09	2.27	0.495	0.257	25.3	357	8.4	16.9	167	117	127	328	303
12-200	50.37	2.559	13.40	11.95	0.17	7.38	11.08	2.33	0.508	0.258	25.5	356	8.7	17.3	165	115	128	337	304
12-201	49.98	2.555	13.22	11.97	0.17	7.45	11.02	2.28	0.507	0.257	25.7	355	8.8	17.7	164	116	137	350	296
12-202	50.23	2.575	13.30	12.02	0.17	7.24	11.08	2.29	0.494	0.258	25.7	362	8.1	16.0	166	113	126	335	291
12-203	50.03	2.559	13.33	12.01	0.17	7.43	11.02	2.20	0.492	0.257	25.7	355	8.3	16.7	165	118	142	341	303
13-209	50.37	2.550	13.45	11.92	0.18	7.25	11.11	2.41	0.499	0.260	25.6	360	8.3	16.4	169	117	125	324	305
13-216	50.03	2.555	13.27	11.96	0.17	7.28	11.11	2.23	0.490	0.253	25.7	358	8.3	16.1	172	118	123	319	308
13-224	50.06	2.561	13.33	11.95	0.17	7.21	11.12	2.29	0.498	0.259	25.5	356	8.5	16.6	165	147	122	319	303
13-225	50.04	2.554	13.34	11.96	0.17	7.16	11.13	2.25	0.491	0.254	25.4	356	8.2	17.1	168	116	121	323	303
14-229	50.29	2.552	13.42	11.97	0.17	7.29	11.13	2.29	0.493	0.255	25.8	354	8.5	16.5	167	117	127	334	299
14-232	50.51	2.562	13.45	12.05	0.17	7.32	11.19	2.29	0.497	0.256	25.6	356	7.9	16.7	166	119	128	329	306
15-237	50.44	2.553	13.41	12.06	0.17	7.36	11.16	2.34	0.500	0.277	25.9	353	8.5	18.1	165	115	126	331	300
16-246	50.33	2.525	13.39	11.98	0.17	7.38	11.14	2.34	0.482	0.252	24.8	352	7.9	17.3	163	114	125	337	303
16-247	50.09	2.520	13.30	11.97	0.17	7.34	11.12	2.26	0.482	0.252	25.0	352	8.1	18.0	163	116	132	336	297
16-254	50.12	2.520	13.31	12.06	0.17	7.43	11.13	2.21	0.481	0.257	25.2	354	8.2	17.9	166	117	133	339	299
17-256	50.12	2.517	13.28	11.98	0.17	7.39	11.14	2.18	0.476	0.252	25.2	352	8.0	18.8	162	115	131	338	293
17-260	50.13	2.511	13.30	11.98	0.17	7.44	11.13	2.26	0.479	0.250	25.0	354	8.5	20.5	162	117	131	338	299
18-263	50.06	2.504	13.30	11.95	0.17	7.48	11.11	2.34	0.475	0.247	24.9	353	8.0	—	155	115	131	336	288
18-269	50.15	2.493	13.29	12.00	0.17	7.51	11.14	2.29	0.475	0.249	24.7	352	8.4	15.8	160	113	129	337	289
20-274	50.41	2.489	13.37	11.96	0.17	7.59	11.14	2.26	0.482	0.251	25.1	363	8.2	17.0	161	119	134	348	301
22-283	49.90	2.490	13.17	11.95	0.17	7.51	11.09	2.15	0.478	0.246	24.6	348	7.7	—	155	116	131	347	289
25-315	50.09	2.477	13.23	12.01	0.17	7.52	11.12	2.22	0.469	0.247	24.9	351	7.7	15.2	156	112	130	349	289
25-325	50.03	2.471	13.15	12.02	0.17	7.66	11.10	2.23	0.468	0.245	24.6	347	8.0	16.2	158	109	137	366	293
26-332	50.31	2.482	13.30	12.00	0.17	7.72	11.17	2.10	0.474	0.248	25.3	351	8.0	15.1	157	115	131	359	295
26-333	50.23	2.473	13.27	12.01	0.17	7.65	11.14	2.22	0.468	0.244	24.8	349	8.8	15.6	158	111	134	356	287
28-337	50.02	2.474	13.17	12.05	0.17	7.63	11.11	2.23	0.471	0.247	25.0	351	8.3	16.6	158	112	128	354	288
29-350	50.30	2.488	13.31	12.03	0.17	7.53	11.13	2.32	0.474	0.249	24.7	351	7.9	16.7	157	110	124	341	287
29-356	49.82	2.464	13.08	12.11	0.17	7.65	11.08	2.23	0.468	0.246	25.1	349	8.3	15.4	157	110	137	364	286
30-359	50.20	2.483	13.26	12.07	0.17	7.51	11.15	2.23	0.472	0.248	25.3	350	8.1	16.2	156	112	124	341	288
30-361	49.81	2.385	12.78	12.25	0.17	8.93	10.76	2.22	0.449	0.240	23.7	338	7.6	15.0	149	111	187	465	272
30-362	49.61	2.346	12.58	12.32	0.17	9.43	10.62	2.19	0.443	0.233	23.7	331	7.8	15.6	148	112	227	544	280
31-363	50.06	2.460	13.20	12.07	0.17	7.71	11.09	2.29	0.465	0.244	25.5	350	7.8	16.7	158	112	133	371	302
31-367	49.89	2.400	12.78	12.33	0.17	8.92	10.77	2.24	0.453	0.238	24.5	340	7.4	14.9	149	109	183	468	274
31-368	49.56	2.347	12.55	12.39	0.18	9.47	10.62	2.17	0.442	0.233	23.7	330	7.6	14.9	149	113	216	567	277
32-370	50.30	2.463	13.25	12.08	0.17	7.71	11.10	2.30	0.472	0.248	24.9	343	7.7	15.3	159	116	132	355	292
35-394	50.25	2.473	13.22	12.14	0.17	7.69	11.04	2.28	0.475	0.249	25.1	345	8.1	15.4	159	119	133	369	291
35-419	50.20	2.470	13.21	12.13	0.17	7.61	11.09	2.17	0.470	0.247	25.0	348	8.5	15.6	163	124	127	363	290
38-458	50.21	2.458	13.23	12.11	0.17	7.66	11.09	2.25	0.465	0.246	25.2	341	8.2	15.7	162	124	125	360	291

For continuation of table 3 please see next page

Table 3 (continued)

Sample	SiO_2	TiO_2	Al_2O_3	Fe_2O_3	MnO	MgO	CaO	Na_2O	K_2O	P_2O_5	Y	Sr	Rb	Nb	Zr	Zn	Ni	Cr	V
40–484	50.08	2.454	13.21	12.04	0.17	7.45	11.05	2.26	0.473	0.244	25.4	343	8.0	16.5	157	116	119	339	294
42–514	50.19	2.463	13.23	12.10	0.17	7.56	11.06	2.21	0.471	0.244	24.7	343	7.9	15.9	162	124	119	350	296
46–536	50.22	2.474	13.24	12.23	0.17	7.54	11.10	2.33	0.465	0.246	25.3	343	7.7	16.2	161	119	122	355	305
46–542	49.98	2.449	13.14	12.17	0.17	7.59	11.03	2.27	0.462	0.242	24.8	341	7.7	16.4	154	115	125	362	296
46–549	50.06	2.458	13.18	12.18	0.17	7.59	11.05	2.27	0.462	0.241	25.0	341	7.8	16.3	156	116	122	361	296
47–570	50.40	2.473	13.33	12.21	0.17	7.66	11.10	2.23	0.470	0.248	25.2	342	7.3	15.1	163	116	120	344	293

Table 4. Results from least-square calculations modeling the magmatic evolution of the Puu Oo reservoir. The model involves mixing of mafic magma delivered from the summit reservoir (assumed to be the most mafic Puu Oo lava, sample 31–368) and the early hybrid lava (the composition of sample 3–96 is used as representative of the hybrid) with minor fractionation of olivine to form the most mafic lava from episodes 3–10 and 30. Olivine in these lavas contains Cr-spinel inclusions, so a mixture of 98.5% olivine of forsterite 83 composition (a typical composition in these lavas) and 1.5% Cr-spinel was used (following the procedure of Wright 1971). Time refers to days since last eruption

New lava	3–88	4–130	5–139	6–154	7–167	8–174	9–178	10–187	30–362
MgO wt %	6.7	7.1	8.1	8.3	7.8	7.9	8.2	8.4	9.4
Time (days)	24	65	12	19	21	20	8	17	31
Mafic magma %	34.5	48.8	67.0	69.8	76.5	77.6	81.7	84.7	100.2
Early hybrid %	67.0	52.6	33.6	30.7	25.1	24.4	20.1	16.8	—
Olivine %	− 1.5	−1.6	−0.6	−0.5	−1.6	−2.0	−1.8	−1.5	− 0.2
$\sum$ Residuals^2 for major elements	0.03	0.05	0.03	0.05	0.06	0.04	0.05	0.03	0.00
Trace elements residual (observed - calculated) in ppm									
Zr (2.5)*	− 1	2	−2	−1	5	1	4	5	1
Rb (1)	0	0	−1	0	0	0	0	0	0
Sr (7)	4	−3	−1	−2	−3	−2	−1	−1	0
V (10)	1	2	6	−5	2	−5	0	6	2
Cr (8)	−12	22	36	10	39	17	37	8	−18
Ni (4)	1	8	22	10	34	14	14	6	11

* 4σ of analytical precision (from Rhodes 1988)

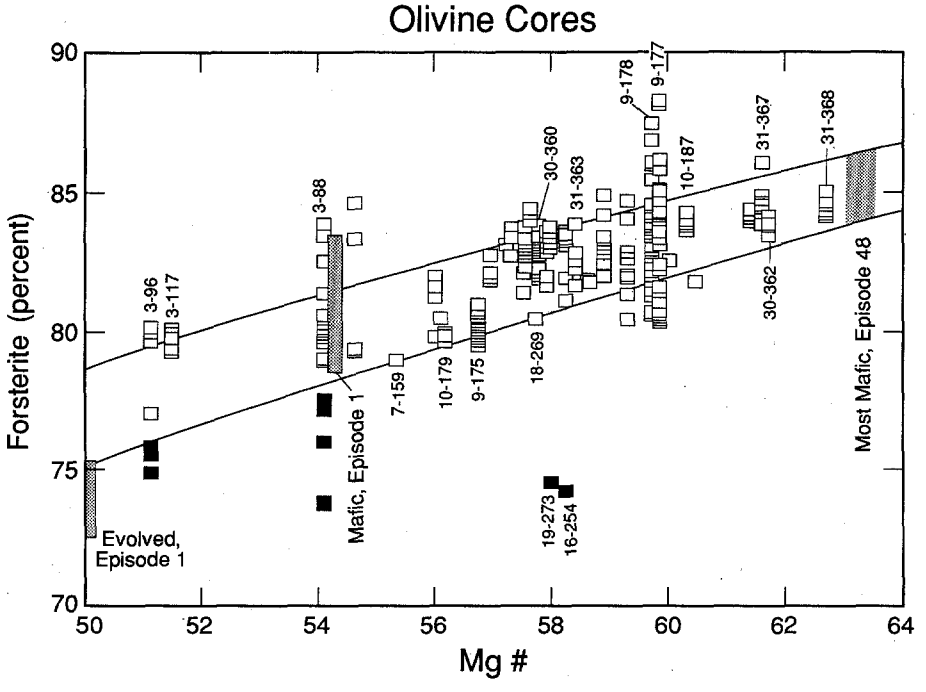

Fig. 2. Mg number of whole rock (assuming $Fe^{2+} = 0.9$ Fe total) versus % forsterite content of the cores of olivine phenocrysts and microphenocrysts from lavas from the Puu Oo eruption. Multiple analyses are shown for most samples. *Solid boxes* are reversely zoned grains. *Open boxes* are unzoned or normally zoned. Fields are shown for the olivines from the evolved and mafic lavas from the first episode (*stippled bars*; Garcia et al. 1989) and most mafic lavas from the 48th episode (*stippled area*) of the Puu Oo eruption. Selected samples from episodes 3–31 are labeled. All post-episode 19 analyses plot within the equilibrium field of Roeder and Emslie (1970; two parallel lines)

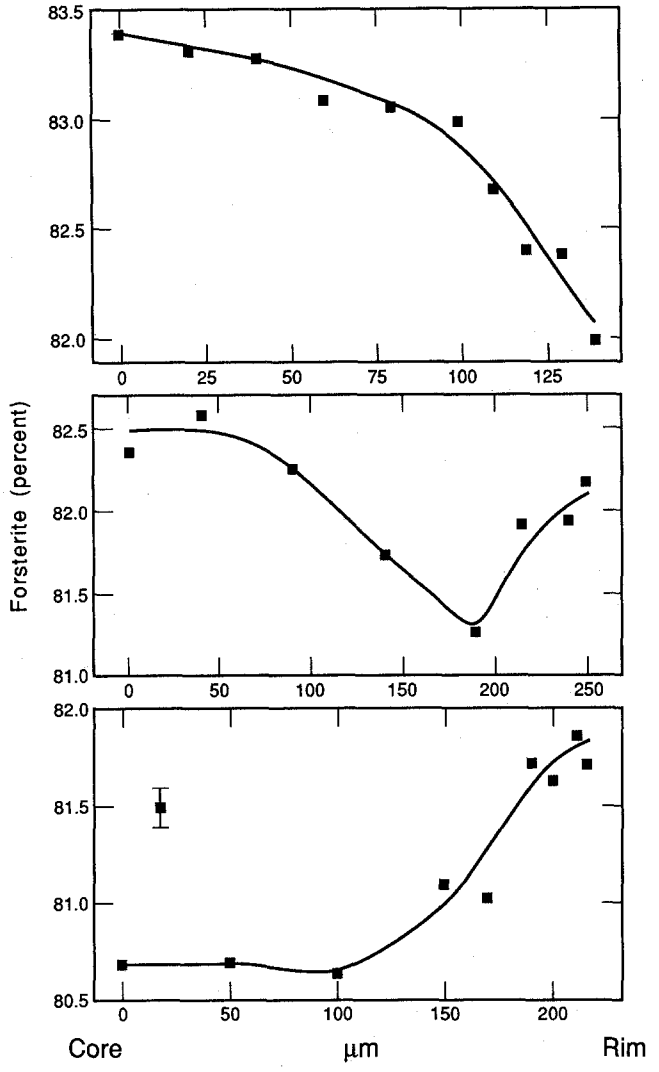

Fig. 3. Profiles of the variation in % forsterite content with distance (in microns) from the core to rim of two olivine phenocrysts and a microphenocryst from sample 9-178. The upper panel shows normal zoning; the lower two panels show reversed zoning. The olivine with the highest forsterite content has normal zoning. Although the compositional variation is small (~1.5% Fo),it is well outside of analytical error (2 sigma error bar shown in lower panel)

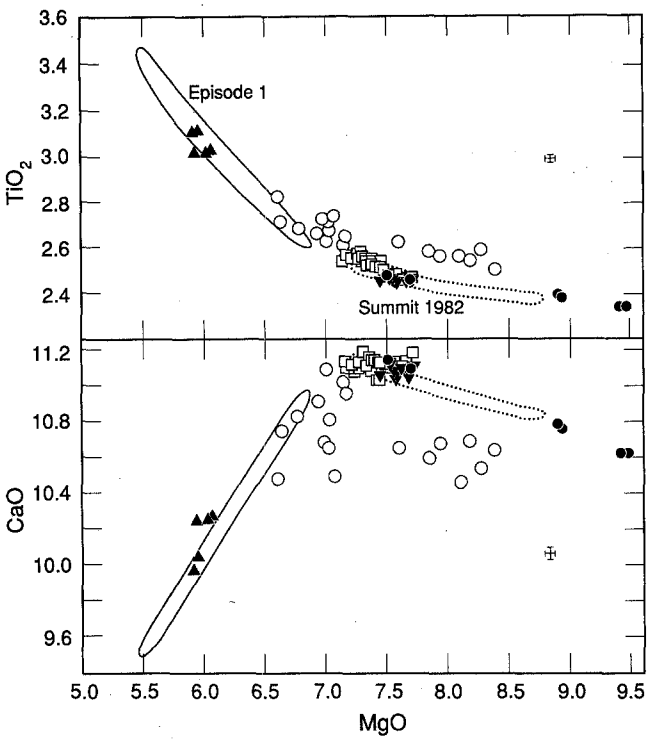

Fig. 4. MgO variation diagram for TiO_2 and CaO for episode 2–47 lavas from the Puu Oo eruption. Also shown are fields for lavas from episode 1 of the Puu Oo eruption (Garcia et al. 1989) and the September 1982 summit eruption of Kilauea (Baker 1987). Symbols: *solid triangles,* episodes 2 and 3 lavas (not from Puu Oo vent); *open circles,* Puu Oo vent lavas from episodes 3–10; *open boxes,* lavas from episodes 11–29; *solid circles,* episodes 30 and 31; *inverted solid triangles,* episodes 32–47

tionation) versus time (Fig. 6). The ratio increases steeply between episodes 3 and 12, gradually between episodes 14 and 25, and then remains relatively constant afterwards. Superimposed on these long-term trends is a short-term cyclic variation of episodes 5–10, 30 and 31 (Fig. 6) when the lavas became progressively more mafic during each episode.

Causes of compositional variation

Overview

Repeated magma intrusions have occurred in the east rift zone of Kilauea (e.g. Klein et al. 1987). Many of these injections were accompanied by seismic swarms caused by the forceful injection of dikes through country rock (Rubin and Pollard 1987). Local magma bodies from such intrusions may be isolated from each other within the rift zone and have different compositions (Wright and Fiske 1971). These compositional differences could reflect derivation from chemically distinct parental magmas, different degrees of post-intrusion fractionation, and/or mixing of compositionally distinct magmas.

The 1977 east rift zone eruption of Kilauea (Moore et al. 1980) occurred in the same area as the Puu Oo eruption. Fissures from the two eruptions overlap along the strike of the rift zone and are about 200 m apart (Wolfe et al. 1988). Seismic and surface deformation data indicate that a pocket of magma developed in the area of Puu Oo prior to the Puu Oo eruption (Klein et al. 1987; Okamura et al. 1988) and that a new dike of magma intruded into the same area the day before the Puu Oo eruption began. The petrology of the lavas from the Puu Oo eruption allows us to evaluate whether these magmas were chemically distinct and, in combination with field and geophysical data, to constrain the location and mechanics of mixing of magma from different reservoirs in the rift zone.

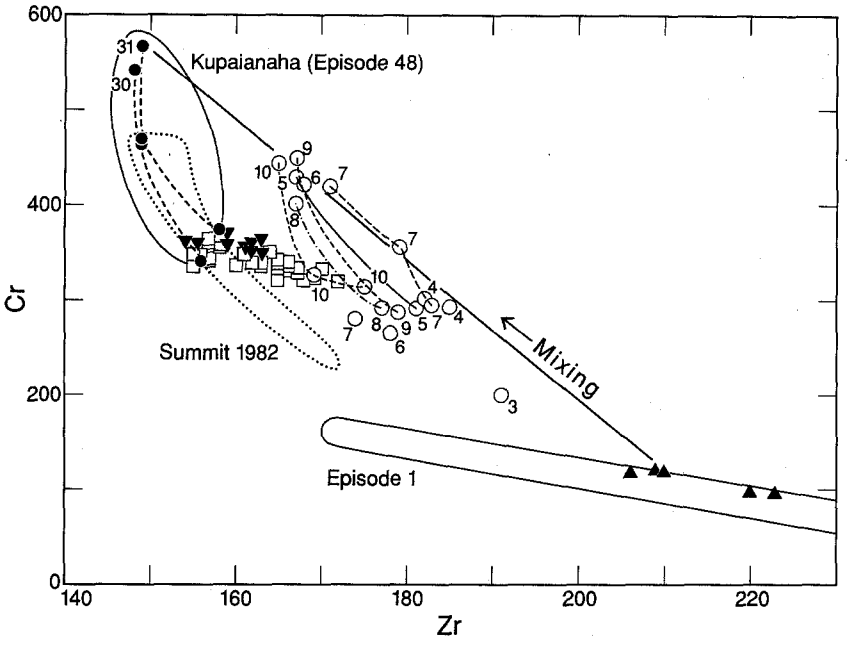

Fig. 5. Zr versus Cr plot for lavas from the Puu Oo eruption. Also shown are fields for lavas from the September 1982 summit eruption (Baker 1987), and episodes 1 (Garcia et al. 1989) and 48 of the Puu Oo eruption (Garcia and Rhodes, unpubl.). A *mixing line* connects the early hybrid lavas from episode 3 with the mafic lavas from episodes 30 and 31. *Dashed lines* connect samples from the same episode. *Numbers* correspond to episode number. The first three-component lava is shown by the *open circle with a 3*. Symbols as in Fig. 4

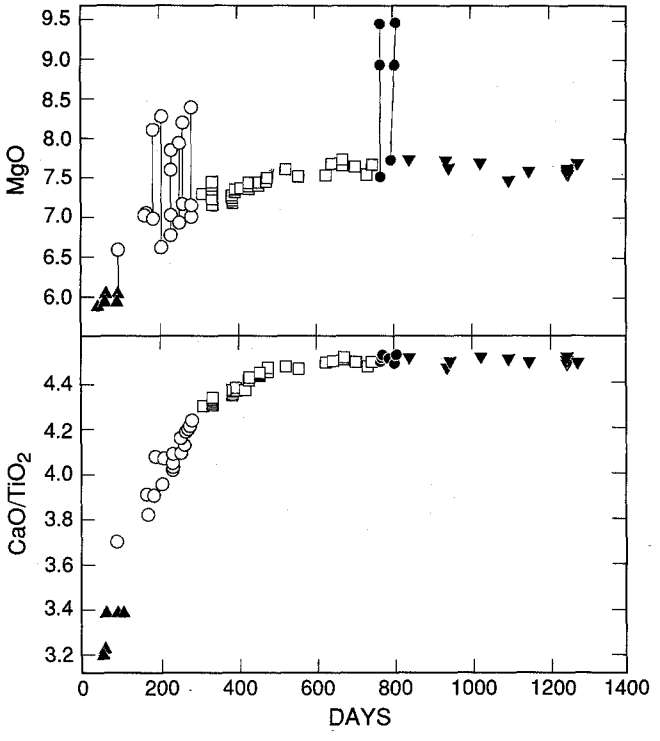

Fig. 6. Variation of MgO (wt %) and CaO/TiO_2 ratio with time (days since start of the Puu Oo eruption). Tie-lines connect samples from the same episode in the MgO plot. Symbols as in Fig. 4

Short-term compositional variation

Compositions within several individual eruptive episodes (5–10, 30 and 31) vary progressively from early evolved lava to later more mafic lava. Although most of these lavas (except from episodes 30 and 31) display mineralogical signs of mixing (e.g. reverse zoning), the short-term compositional variation is probably largely controlled by crystal fractionation between eruptions. Systematic changes in mineral proportions and compositions during individual episodes (Tables 1 and 2) are consistent with crystal fractionation. For example, each sample from episodes 30 and 31 has a distinct compositional range for olivine that is in equilibrium with the host rock (Fig. 2). Least-squares calculations indicate that the overall compositional variation for episodes 30 and 31 can be satisfactorily explained (ΣR^2 for major elements = 0.001 and 0.018, respectively) by 4.7 and 4.9% fractionation of olivine (with 1.5% Cr-spinel). However, the modal variation of olivine (phenocrysts and microphenocrysts) is only about 1 vol % (Table 1). Thus, the observed compositional variation cannot be due simply to accumulation of olivine in a low MgO lava.

The apparent rate of fractionation in the Puu Oo reservoir can be determined using: (1) least-squares calculations for the extent of crystal fractionation between the mafic lavas from the end of episodes 30 and 31 and the evolved lavas from the beginning of episodes 31 and 32; and (2) the duration of the repose periods between these episodes (36.2 and 38.5 days). This rate is high (1% per eight days) compared to previous estimates of fractionation in Kilauea's east rift zone (e.g. 1–2% per year; Wright and Tilling 1980). However, as emphasized by Wright and Tilling (1980), many factors may influence the crystallization rate. For Puu Oo, the geometry of the shallow magma reservoir and its open top are the key factors. A surface deformation study conducted between episodes 22 and 42 found that the Puu Oo magma reservoir was a shallow (0.4–2.9 km deep), narrow dike about 3 m wide, 1.6 km long and 2.5 km high (Hoffmann et al. 1990). The large surface area to volume aspect of this reservoir would promote rapid crystallization. Rapid crystallization was further enhanced by the open top of the magma reservoir (see Wolfe et al. 1988), which facilitated loss of heat and volatiles. Normally,

the vent in Puu Oo crater was an open pipe averaging 20 m in diameter. Thus, the conditions were ideal in the Puu Oo magma reservoir for high rates of crystallization during the short intervals (8–52 days) between eruptions. This led to the formation of a compositionally zoned reservoir beneath Puu Oo. The upper part of this reservoir contained evolved magma that was erupted at the beginning of all episodes; the lower part of the reservoir system contained more mafic magma.

Mafic magma was not erupted during episodes 11–29 and 32–47. Apparently the volume of lava erupted during those episodes was insufficient to tap the more mafic portions of the reservoir. However, there is no simple correlation between the volume of lava erupted during an episode and the range of compositional variation of the lava. For example, episode 18 was the most voluminous eruption from the Puu Oo vent (24 million m^3), but lavas from that episode exhibit only a small compositional range (Table 3). The volume of evolved magma erupted during this episode is 18 million m^3, when corrected for vesicularity (estimated to be on average about 25%; Wolfe et al. 1987). This is somewhat larger than the minimum estimate of 10–12 million m^3 for the volume of the Puu Oo reservoir given by Hoffmann et al. (1990). If the reservoir was 4.5 m wide, instead of the 3 m estimated by Hoffmann, it could accommodate this volume. This would require a 25% increase in width from that of the initial feeder dike (3.6 m; Dvorak et al. 1986).

Long-term compositional variation

The lavas erupted during episode 1 of the Puu Oo eruption are mostly hybrids that were produced by mixing two differentiated, rift-zone-stored magmas (Garcia et al. 1989). The mixing of these two magmas to produce what we subsequently call the 'early hybrid' was probably triggered by the intrusion of a dike just before the eruption started in 1983 (Fig. 7). This dike was the progenitor of a conduit that has delivered mafic magma from the summit reservoir to the rift zone near Puu Oo from 1983 through to mid 1992. The most likely sources of the rift-zone-stored magmas erupted during episode 1 are the evolved magma reservoir that fed the 1977 eruption and a pocket of less-evolved magma that formed prior to 1983 in the Puu Oo area (Garcia et al. 1989).

Additional early hybrid lava was erupted from fissures during episode 2 (Wolfe et al. 1987). During episode 3, two central vents were active. At the uprift vent

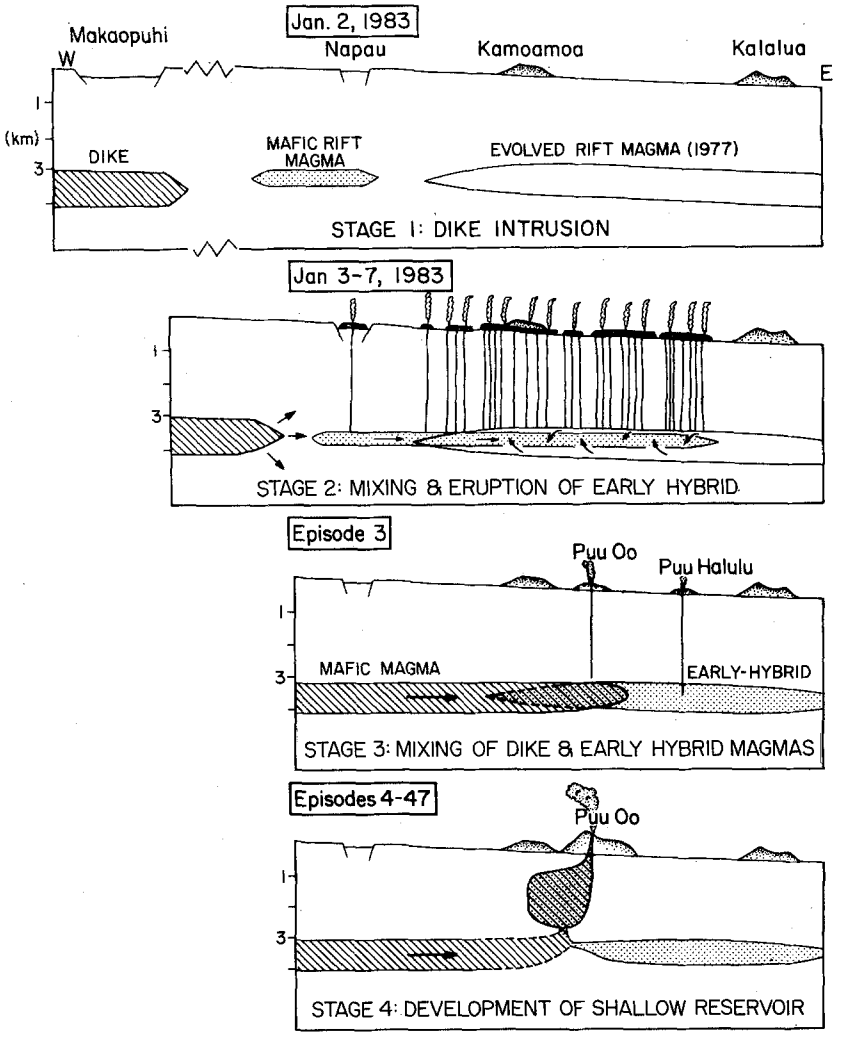

Fig. 7. Cartoon sequence of cross sections depicting the temporal evolution of the Puu Oo magma reservoir system. See text for constraints used in constructing the cartoon. The prehistoric cones, Kamoamoa and Kalalua, and pit craters, Makaopuhi and Napau, are shown for scale

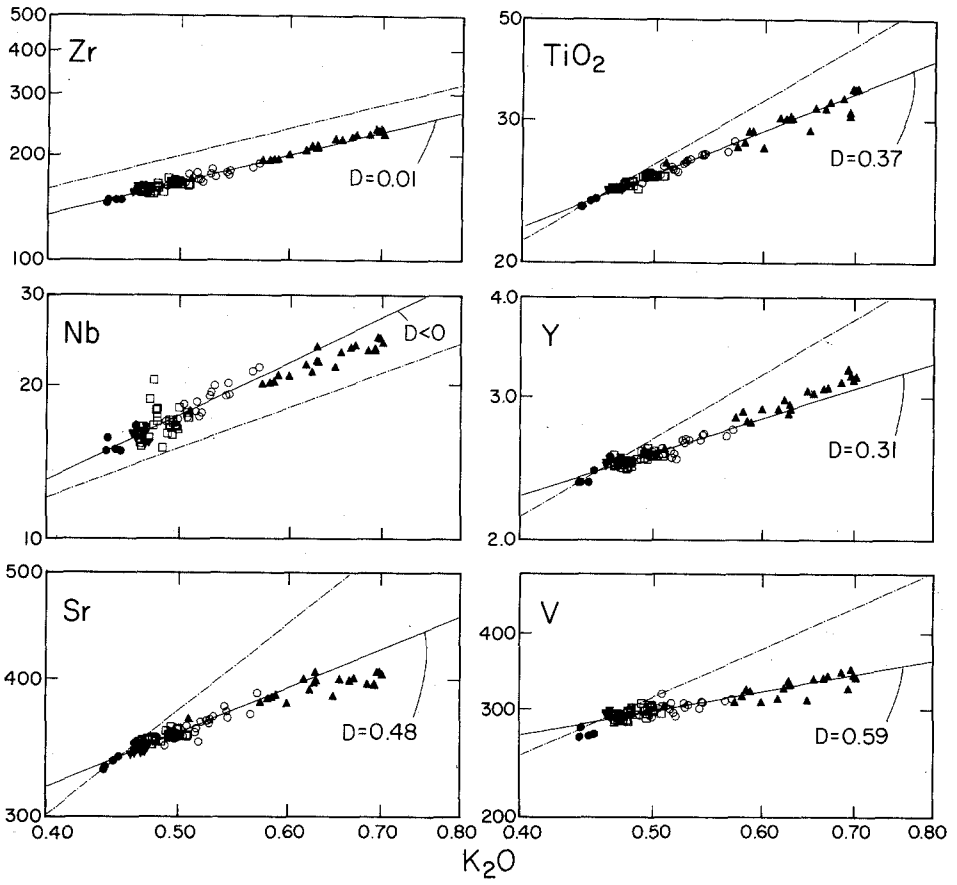

Fig. 8. Log-log plots of K_2O (in wt %) versus Zr, Nb, Sr, Y, V (all in ppm) and TiO_2 (in wt %) for Puu Oo lavas. These elements are normally highly incompatible in Kilauea lavas. Symbols: *solid diamonds,* lavas from episodes 1 and 2; others as in Fig. 4. The apparent bulk distribution coefficient (*D*) for each element was calculated from the slope of the best-fit line (*solid*) through data for samples from episodes 3–47 only. The *dashed-dot line* shows the slope of the line assuming both elements have a bulk distribution coefficient equal to zero

(where Puu Oo later formed), somewhat more mafic lava was erupted. The composition of this lava, sample 3-88, plots off the mixing trend for the lavas erupted during the first two episodes and from the other episode-3 vent (Puu Halulu; see Fig. 5). Thus, a different, more mafic magma entered the Puu Oo magma reservoir system prior to the start of episode 3 (Fig. 7).

During episodes 4–47, lava erupted only from or near the Puu Oo vent. The composition of the lava erupted from the Puu Oo vent became progressively more mafic during the first year (Fig. 6). We propose that this was caused by the progressive increase in the percentage of mafic magma being mixed with the early hybrid magma. A mixing line can be drawn between the compositions of the early hybrid lavas erupted from the Puu Halulu vent during episode 3 and the most mafic lavas sampled during episodes 30 and 31 (Fig. 5). The more mafic lavas of the compositional variable episodes (5–10, 30 and 31) plot along this mixing trend. All other lavas from episodes 5 through 47 plot off this trend, presumably because olivine (with minor Cr-spinel) fractionation in the shallow reservoir removed Cr from the magma.

The most mafic Puu Oo lavas were erupted about two years after the start of the eruption at the end of episodes 30 and 31. The composition of the lava erupted during these episodes is similar to that of lavas erupted during the September 1982 summit eruption of Kilauea and the continuous eruption (1986 to present) from the Kupaianaha vent (Figs. 4 and 5). This compositional similarity supports the geophysical evidence that the Puu Oo eruption was supplied with magma from the summit reservoir (Wolfe et al. 1987).

The relative importance of magma mixing versus crystal fractionation can be evaluated by log-log diagrams of element distribution patterns (e.g. Allègre et al. 1977; Cocherie 1986). Compositional variations produced by fractional crystallization plot along linear trends with slopes that are proportional to the bulk distribution coefficients (*D*) of the elements involved:

$$Slope = (D_1 - 1)/(D_2 - 1)$$

If the *D*s remain constant, and one of the elements is highly incompatible such that $D_2 \approx 0$, then the bulk distribution for the other element (*D*) is approximated by (1 − slope). Conversely, if the other element is also incompatible, then the trend will have a slope that is close to one. This useful relationship can be used to evaluate magmatic processes in the Puu Oo lavas.

Figure 8 shows log-log relations for several elements in Puu Oo lavas that are normally incompatible in Kilauea lavas. They are plotted against K_2O, which is assumed to be highly incompatible. If these trends result from crystal fractionation, then, given the low proportion of phenocrysts and the nature of the phenocryst phases in these lavas (Table 1), most of the elements evaluated (Rb, Sr, Nb, Zr, Y, Ti and V) should behave as incompatible elements, forming linear trends with K_2O, with slopes close to unity. Although the data define linear trends consistent with fractional crystallization, the slopes are highly variable ranging from a low

of 0.41 for V to a high of 1.33 for Nb. Only Zr has a slope that is close to one and behaves as a highly incompatible element. Most of the other elements that are normally highly incompatible in Kilauea lavas have lower slopes, indicative of relatively high bulk partition coefficients (e.g. $D_{Sr}=0.48$; $D_Y=0.31$; $D_{Ti}=0.37$; $D_V=0.59$). Such 'apparent' D values require *extensive* fractionation of plagioclase (Sr), clinopyroxene (Ti, Y) and opaques (Ti, V) for the entire suite of Puu Oo lavas. This inference is at odds with the observed phenocryst assemblage, especially the post-episode 13 lavas (Table 1). Even more problematical are plots of Nb and Rb against K_2O, which have slopes greater than one. This is an impossible situation if the trends result from fractional crystallization, because D cannot be negative. These log-log relationships imply either that fractional crystallization is not responsible for the observed trends in these lavas, or that K_2O is an inappropriate choice for the incompatible reference element.

All of the elements inferred to have relatively high D values *are* elements that are partitioned into minerals such as plagioclase, clinopyroxene and ilmenite or magnetite. These minerals crystallize after olivine in Kilauea magmas, at temperatures below 1160° C, as the melt cools and evolves (Helz and Thornber 1987). Of particular importance is V, which is strongly partitioned into magnetite and ilmenite. These opaque minerals are absent from the glassy Puu Oo lavas (Table 1). Typically, they crystallize only in strongly evolved Kilauea magmas (e.g. 1977 lavas with MgO ~5.3 to 5.8 wt %; Moore et al. 1980). The elements inferred to have low, or impossible, D values (Rb, Zr, Nb) should be highly incompatible throughout this entire temperature and compositional range. The paradox is resolved if the linear log-log trends result from mixing a highly evolved magma with more primitive incoming magma. Crystallization of plagioclase, clinopyroxene and opaque minerals has occurred, but in the evolved melt prior to mixing. Similarly, slopes greater than one will occur if the K/Rb and K/Nb ratios of the mixed magmas are not the same.

Nature of magma mixing in the Puu Oo magma reservoir

Components and mechanics

Several simple models were evaluated to understand the mechanics of the mixing process in the Puu Oo reservoir and to constrain the geometry of the various magma bodies in the rift zone in the Puu Oo area. Our petrologic examination of lavas from episodes 3–47 indicates that some are hybrids produced by mixing mafic and evolved magmas. Least-squares calculations were made to determine the most likely mixing components for the mafic lavas from several episodes (Table 4). The mafic Puu Oo lavas were modeled because the evolved lavas have the additional effects of substantial crystal fractionation of several different minerals. For the mixing components, we used the composition of the most mafic Puu Oo lava (sample 31–368) to approximate the mafic magma composition. It contains no petrographic evidence of magma mixing, and the olivine phenocrysts in the lava are in equilibrium with the whole rock composition (see Fig. 2). The most evolved lava from episode 3 (sample 3–96 from Puu Halulu; Fig. 7) was used to represent the early hybrid composition. Its composition is within the range of those erupted during episodes 1 and 2, and it plots on the mixing trend for those lavas. Because olivine and Cr-spinel are the liquidus minerals in these rocks, we assumed that there might have been some minor fractionation of these phases prior to, accompanying, and following mixing.

The shape and size of the Puu Oo magma reservoir is an important constraint in our petrological modeling. The ground deformation study of Hoffman et al. (1990) indicates that the reservoir is dike shaped, about 1.6 km in length, 2.6 km in depth and about 3 m wide, and grew in size from about 3 million m^3 during the early eruptive episodes to at least 18 million m^3 in later episodes. This volume is similar to that erupted during many of the episodes (Wolfe et al. 1987; Hoffman et al. 1990). Thus, our modeling assumed that most or all of the magma in the shallow Puu Oo reservoir was erupted during each episode and that fractionation would occur in the reservoir between eruptions. Our basis model assumed that the magma in the Puu Oo reservoir was a mixture of mafic magma derived from a dike that tapped the summit reservoir and the early hybrid magma that was erupted during episodes 1–3.

The more mafic lava from episode 3 (sample 3–88, erupted from the Puu Oo vent) can be explained by mixing 34.5% of the mafic magma with 67.0% evolved early hybrid magma, accompanied by 1.5% olivine fractionation. This combination yields excellent residuals (Table 4). Modeling the most mafic lavas from episodes 5–10 and 30 also yielded good to excellent results for all elements but Cr and Ni (Table 4). This may be due to different ratios of olivine to Cr-spinel in the rocks compared to those used in the modeling (98.5% olivine to 1.5% Cr-spinel, an average ratio for Kilauea lavas; Wright 1971). Also, only minor variations (0.1 vol %) in the abundance of olivine (with its inclusions of Cr-spinel) are needed to explain these high residuals.

Solutions for modeling the mafic lavas from episodes 5–10 require variable but small amounts of olivine and Cr-spinel fractionation (0.2 to 2.0%; Table 4). However, there is no correlation of the amount of fractionation indicated by the least-squares calculations and the duration of the hiatus preceding the eruption (Table 4) or the volume of lava erupted during the previous episode. This lack of correlation is probably related to the variable volumes of lavas erupted during each episode, which resulted in the most mafic lava from each episode representing different levels within the reservoir (i.e. different percentages of fractionation).

Timing

The model proposed above predicts several different mixing events. The timing of the mixing events can be

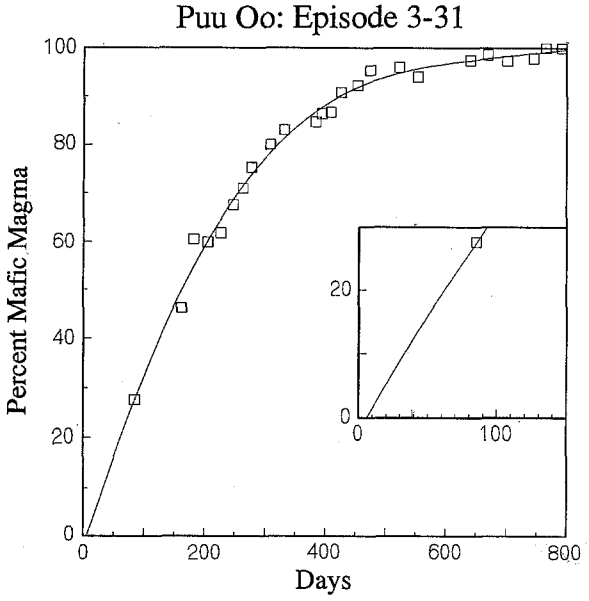

Fig. 9. Temporal variation in the % mafic magma component in the lavas erupted from the Puu Oo vent. The % mafic magma component is calculated using the CaO/TiO_2 ratio of lavas from episodes 3–31, with the early-hybrid lava sample 3–117 and the mafic lava sample 31–368 as endmembers. A 5th order polynomial regression line was fitted to data to estimate when mixing began. Lower order polynomial regressions produced unsatisfactory fits to the data. A blowup of the x-intercept (i.e. 0% mafic magma) for the line is shown in the insert

constrained from our petrologic results and from ground deformation studies (Okamura et al. 1988; Hoffmann et al. 1990). The mixing that produced the early hybrid from the two rift-zone-stored magmas probably occurred just before the start of the Puu Oo eruption when the mafic dike was intruded (Garcia et al. 1989). When did the mafic magma from this dike start mixing with this hybrid? Ground deformation (Okamura et al. 1988) and seismicity (Wolfe et al. 1987; Koyanagi et al. 1988) indicate that the dike intruded into the Puu Oo area the day before the eruption started. However, the first lava with clear compositional indications of the mafic magma from this dike was not erupted until the 85th day of the eruption and was erupted only from the Puu Oo vent. It should be noted that no lava was collected from the Puu Oo vent during episode 2. Thus, it is uncertain exactly when the mixing with the mafic magma began.

The CaO/TiO_2 ratio can be used to estimate when mixing began and terminated (i.e. 100% mafic magma in the erupted lava). This ratio is distinct for the two mixing components (Fig. 6) and is virtually unaffected by olivine fractionation. The first collected, three-component hybrid lava (sample 3–88) has 27.6% mafic magma. The concentration of mafic magma in the erupted lavas increased rapidly during the first 310 days of the eruption to 80%. The rate of increase then slowed gradually to where lavas of episodes 25–29 (626–746 days after the start of the eruption) have only minor early hybrid components (1–2%; see Fig. 9). The episode 30 lavas, erupted 764 days after the start of the eruption, contain only the mafic component and mark the end of mixing between the mafic magma and the early hybrid magma. This is consistent with the presence of reversely zoned minerals in lavas from only episodes 1–19. Thus, mixing occurred through at least episode 19.

To estimate the beginning of mixing, we used a 5th order polynomial regression of the data to generate a curve that we projected to 0% mafic component (Fig. 9). Lower order polynomials regressions yielded less satisfactory fits to the data. This approach assumes that mixing was continuous and progressive. The R^2 for the polynomial equation is 0.990. The difference in the polynomial regression curve and the data is <1 day to 7 days. The curve projects to about 8 days after the start of the eruption. However, a lava (sample 1–54; Garcia et al. 1989) erupted at the end of episode 1 (21 days after the start of the eruption) from a vent where the Puu Oo later formed has essentially the same CaO/TiO_2 ratio as the early hybrid endmember. Thus, the three-component hybrid was not erupted in the Puu Oo area during the first 21 days of the eruption. Perhaps mixing began just after the end of episode 1, 25–30 days after the start of the eruption. The difference between the predicted and the earliest possible day when mixing could have started may be related to the discontinuous nature of the mixing events during and following each eruptive episode.

Mixing also occurred sometime during or after each eruptive episode. Deformation studies indicate that during the repose intervals between eruptive episodes 21 and 42, the dike-shaped Puu Oo reservoir expanded due to the flux of new magma into the reservoir (Hoffmann et al. 1990). Borehole-tiltmeter data (Wolfe et al. 1987) indicate that each influx occurred gradually and steadily throughout the repose period. Using the dimensions of the dike reservoir estimated from the deformation work, the volume of magma entering the reservoir between eruptions was 150–915 thousand m^3 (Hoffmann et al. 1990). This volume is small (1.6–8.6%) compared to that erupted during an episode. Thus, the bulk of the magma that recharged the Puu Oo reservoir was not intruded during repose intervals between eruptions. The rapid subsidence of the summit reservoir during a Puu Oo eruption (Wolfe et al. 1987) indicates that replenishment of the Puu Oo reservoir occurred *during* eruptive episodes. Therefore, recharge of magma into the Puu Oo reservoir was episodic, and occurred as pressure was reduced, during or immediately following an eruption.

Geometry of magma reservoir system

The results presented above indicate that the mafic magma from the dike and the early hybrid magma were able to mix readily to create the next batch of magma in the Puu Oo reservoir. Thus, there was a good hydraulic connection between the reservoir and the two magma bodies that recharged it. We can deduce the locations of these three magma bodies from geological and geophysical data. The Puu Oo reservoir was dike shaped and extended 1.6 km uprift from the vent at least during episodes 22–42 (Hoffmann et al. 1990). The early hybrid

magma body is inferred to underlie and extend downrift (east) of the Puu Oo reservoir on the basis of the locations of the vents from which the early hybrid lavas erupted during episodes 1–3. The mafic dike intruded the Puu Oo area from uprift (west) at a depth of 3–4 km (Wolfe et al. 1987). These constraints have been incorporated into a cartoon showing the geometry of the magma bodies in the Puu Oo area (Fig. 7). The locations and nature of the connection between the three bodies of magma are unknown; we have assumed a narrow junction beneath Puu Oo. After episode 29, the connection between the early hybrid reservoir and the rest of the Puu Oo reservoir system was effectively sealed, or the magma was exhausted because no evidence of this magma was detected in post-episode 29 lavas. Thus, only mafic magma from the summit reservoir entered the Puu Oo reservoir after episode 29.

Conclusions

The mineralogy and whole-rock geochemistry of lavas from the Puu Oo eruption of Kilauea Volcano provide insights into the processes that occurred before and during this eruption. The morphology and compositions of the minerals in combination with the lava compositions reveal a history of magma mixing and crystal fractionation. Some of the minerals from the early part of the eruption (prior to episode 20) have reverse zoning and are out of equilibrium with the whole-rock composition. Minerals in later lavas have both equilibrium textures and compositions. The reversely zoned minerals were derived from a hybrid created by mixing of two rift-zone-stored magmas just before the start of the eruption. This 'early' hybrid was erupted during the first three eruptive episodes, and the compositions of these lavas define a linear mixing trend. During episode 3 a new, more mafic hybrid was erupted from a vent where Puu Oo later formed. This was the site of virtually all subsequent eruptive activity until episode 48. For 21 months after episode 3, the lava composition became progressively more mafic as summit-reservoir magma mixed in increasing proportions with the early hybrid magma. However, this three-component hybrid mafic magma fractionated rapidly in the shallow, dike-shaped, reservoir with its open conduit to the atmosphere. Fractionated lava was erupted at the beginning of each eruptive episode and throughout many of them, although during some episodes (5–10, 30 and 31) the lava became progressively more mafic. These observations indicate rapid development of compositional zoning in the shallow Puu Oo magma reservoir during repose periods. The episodes with progressive compositional variation apparently represent occurrences in which the more fractionated magma in the upper part of the Puu Oo reservoir was fully discharged.

Three magma reservoirs were involved in the Puu Oo eruption through episode 29. The shallow (0.4–2.9 km deep) reservoir, with its open vent at Puu Oo, was resupplied with mafic magma from Kilauea's summit reservoir via a conduit within the east rift zone and evolved magma from a reservoir within the rift zone. Recharge of the shallow reservoir occurred rapidly during an eruption indicating that these reservoirs were well connected. The connection with the early hybrid magma body was cut off before episode 30. Subsequently, only mafic magma from the summit reservoir recharged the Puu Oo reservoir.

Acknowledgements. This study would not have been possible without the dedicated sampling efforts of many Hawaiian Volcano Observatory current and former staff members, especially P Greenland, C Heliker, J Hoffmann, J Lockwood, R Moore, T Neal and F Trusdell, and volunteers like S Rowland. Assistance in preparing samples and obtaining XRF and microprobe data by M Chapman, P Dawson, J Hayes, B Martin, E Matsumoto, J Romano, J Sparks and S Spengler are gratefully acknowledged. We thank B Bays, HE Chelette, N Hulbirt and T Hulsebosch for help in preparing figures and Carol Koyanagi for preparing the manuscript. This manuscript benefited from discussions with TL Wright, K Hon, M Mangan and F Trusdell and critical reviews by R Fodor and J Nicholls. This work was supported by NSF grants EAR-8816242 and EAR-9104884 to M. G. This is SOEST contribution no. 2971.

References

Allègre CJ, Treuil M, Minster J-F, Minster B, Albarède F (1977) Systematic use of trace elements in igneous processes. Part I: Fractional crystallization processes in volcanic suites. Contrib Mineral Petrol 60:57–75

Baker NA (1987) A petrologic study of the 1982 summit lavas of Kilauea Volcano, Hawaii. Univ Hawaii, Senior Thesis, 61 pp

Clague DA, Moore JG, Dixon JE, Friesen WB (1992) The mineral chemistry and petrogenesis of submarine lavas from Kilauea's east rift zone, Hawaii. J Petrol (in press)

Cocherie A (1986) Systematic use of trace element distribution patterns in log-log diagrams for plutonic suites. Geochim Cosmochim Acta 50:2517–2522

Delaney PT, Fiske RS, Miklius A, Okamura AT, Sako MK (1990) Deep magma body beneath the summit and rift zones of Kilauea Volcano, Hawaii. Science 247:1311–1316

Dvorak JJ, Okamura AT, English TT, Koyanagi RY, Nakata JS, Sako MK, Tanagawa WT, Yamashita KM (1986) Mechanical response of the south flank of Kilauea Volcano, Hawaii, to intrusive events along the rift systems. Tectonophysics 124:193–209

Dzurisin D, Koyanagi RY, English TT (1984) Magma supply and storage at Kilauea Volcano, Hawaii: 1956–1983. J Volcanol Geotherm Res 21:177–206

Fuller RE (1939) Gravitational accumulation of olivine during advance of basalt flows. J Geol 47:303–313

Garcia MO, Wolfe EW (1988) Petrology of the lava. US Geol Surv Prof Pap 1463:127–143

Garcia MO, Ho RA, Rhodes JM, Wolfe EW (1989) Petrologic constraints on rift zone processes: results from episode I of the Puu Oo eruption of Kilauea Volcano, Hawaii. Bull Volcanol 52:81–96

Heliker C, Wright TL (1991) The Puu Oo-Kupaianaha eruption of Kilauea. EOS 72:521–530

Helz RT, Thornber CR (1987) Geothermometry of Kilauea Iki lava lake, Hawaii. Bull Volcanol 49:651–668

Hoffmann JP, Ulrich GE, Garcia MO (1990) Horizontal ground deformation patterns and magma storage during the Puu Oo eruption of Kilauea Volcano, Hawaii: episodes 22–42. Bull Volcanol 52:522–531

Klein FW, Koyanagi RY, Nakata JS, Tanigawa WR (1987) The seismicity of Kilauea's magma system. US Geol Surv Prof Pap 1350:1019–1185

Koyanagi RT, Tanigawa WR, Nakata JS (1988) Seismicity associated with the eruption. US Geol Surv Prof Pap 1453:183–235

Lofgren G (1980) Experimental studies on the dynamic crystallization of silicate melts. In: Hargraves RB (ed) Physics of magmatic processes. Princeton Univ Press, 487–551

Moore RB, Helz RT, Dzurisin D, Eaton GP, Koyanagi RY, Lockwood JP, Puniwai GS (1980) The 1977 eruption of Kilauea Volcano, Hawaii. J Volcanol Geotherm Res 7:189–210

Neal CA, Duggan TJ, Wolfe EW, Brandt EL (1988) Lava samples, temperatures, and compositions. US Geol Surv Prof Pap 1463:99–126

Nicholls J, Stout MZ (1988) Picritic melts in Kilauea – evidence from the 1967–1968 Halemaumau and Hiiaka eruptions. J Petrol 29:1031–1057

Okamura AT, Dvorak JJ, Koyanagi RY, Tanigawa WR (1988) Surface deformation during dike propagation. US Geol Surv Prof Pap 1463:165–181

Rhodes JM (1988) Geochemistry of the 1984 Mauna Loa eruption: implications for magma storage and supply. J Geophys Res 93:4453–4466

Roeder DL, Emslie RF (1970) Olivine-liquid equilibrium. Contrib Mineral Petrol 29:275–289

Rubin AM, Pollard DD (1987) Origins of blake-like dikes in volcanic rift zones. US Geol Surv Prof Pap 1350:1449–1470

Ryan MP (1988) The mechanics and three-dimensional internal structure of active magmatic systems, Kilauea Volcano, Hawaii. J Geophys Res 93:4213–4248

Ryan MP, Koyanagi RY, Fiske RS (1981) Modeling the three-dimensional structure of magma transport system: application to Kilauea Volcano, Hawaii. J Geophys Res 86:7111–7129

Wilkinson JFG, Hensel HD (1988) The petrology of some picrites from Mauna Loa and Kilauea volcanoes, Hawaii. Contrib Mineral Petrol 98:326–345

Wolfe EW, editor (1988) The Puu Oo eruption of Kilauea Volcano, Hawaii: episodes 1 through 20. US Geol Surv Prof Pap 1463, 251 pp

Wolfe EW, Garcia MO, Jackson DB, Koyanagi RY, Neal CA, Okamura AT (1987) The Puu Oo eruption of Kilauea Volcano, episodes 1 through 20, January 3, 1983, to June 8, 1984. US Geol Surv Prof Pap 1350:471–508

Wolfe EW, Neal CA, Banks NG, Duggan TJ (1988) Geologic observations and chronology of eruptive events. US Geol Surv Prof Pap 1463:1–97

Wright TL (1971) Chemistry of Kilauea and Mauna Loa lava in space and time. US Geol Surv Prof Pap 735, 40 pp

Wright TL, Fiske RS (1971) Origin of differentiated and hybrid lavas of Kilauea Volcano, Hawaii. J Petrol 12:1–65

Wright TL, Tilling RI (1980) Chemical variation in Kilauea eruptions 1971–1974. Am J Sci 280-A:777–793

Editorial responsibility: GA Mahood, W Hildreth